Pressure-Sensitive Tissue Adhesion and Biodegradation of Viscoelastic Polymer Blends

John L. Daristotle[1], **Shadden T. Zaki**[2], **Lung W. Lau**[3], **Omar B. Ayyub**[4], **Massi Djouini**[4], **Priya Srinivasan**[3], **Metecan Erdi**[4], **Anthony D. Sandler**[3], **Peter Kofinas**[4]

[1]Fischell Department of Bioengineering, University of Maryland, Room 3102 A. James Clark Hall, 8278 Paint Branch Drive, College Park, Maryland 20742, United States.

[2]Department of Materials Science and Engineering, University of Maryland, 4418 Stadium Drive, College Park, Maryland 20742, United States.

[3]Sheikh Zayed Institute for Pediatric Surgical Innovation, Joseph E. Robert Jr. Center for Surgical Care, Children's National Medical Center, 111 Michigan Avenue NW, Washington, D.C. 20010, United States.

[4]Department of Chemical and Biomolecular Engineering, University of Maryland, 4418 Stadium Drive, College Park, Maryland 20742, United States.

Abstract

Viscoelastic blends of biodegradable polyesters with low and high molecular weight distributions have remarkably strong adhesion (significantly greater than 1 N/cm^2) to soft, wet tissue. Those that transition from viscous flow to elastic, solidlike behavior at approximately 1 Hz demonstrate pressure-sensitivity yet also have sufficient elasticity for durable bonding to soft, wet tissue. The pressure-sensitive tissue adhesive (PSTA) blends produce increasingly stronger pull-apart adhesion in response to compressive pressure application, from 10 to 300 s. By incorporating a stiffer high molecular weight component, the PSTA exhibits dramatically improved burst pressure (greater than 100 kPa) when used as a tissue sealant. The PSTA's biodegradation mechanism can be switched from erosion (occurring primarily over the first 10 days) to bulk chemical degradation (and minimal erosion) depending on the chemistry of the high molecular weight component. Interestingly, fibrosis toward the PSTA is reduced when fast-occurring erosion is the dominant biodegradation mechanism.

Graphical Abstract

Corresponding Author: **Peter Kofinas** – Department of Chemical and Biomolecular Engineering, University of Maryland, College Park, Maryland 20742, United States; kofinas@umd.edu.

Author Contributions
J.L.D., L.W.L., P.S., A.D.S., and P.K. designed the research. S.T.Z., J.L.D., L.W.L., M.D., and O.B.A. performed experiments. J.L.D., S.T.Z., and L.W.L. analyzed results. J.L.D., O.B.A., S.T.Z., A.D.S., and P.K. wrote and edited the manuscript. All authors have given approval to the final version of the manuscript.

Supporting Information
The Supporting Information is available free of charge at https://pubs.acs.org/doi/10.1021/acsami.0c00497.
Thermal data, contact angle measurements, modeling, and surgical images (PDF)
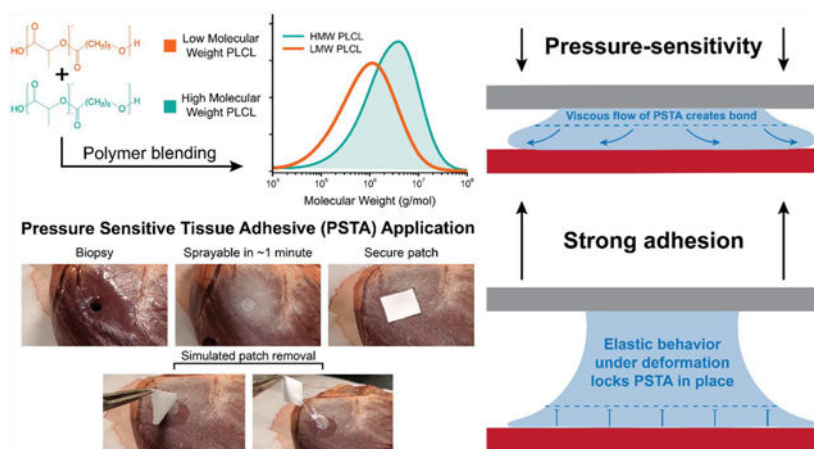
INTRODUCTION

Tissue adhesives can reduce tissue damage by securing organs or biomedical devices noninvasively, potentially eliminating the need for sutures or staples in some surgical procedures. Here, we describe a pressure-sensitive tissue adhesive (PSTA) that can be fixed to intestinal or cardiac tissue simply by applying pressure to the interface, and without any curing event, drastically improving usability. This method employs a bimodal polymer blending strategy to produce an inherently tacky and tissue adhesive polymer film that is also biodegradable, biocompatible, and sprayable. By varying polymer chemistry of the blend, we demonstrate control over the PSTA's viscoelasticity and biodegradation rate, allowing it to be tuned depending on the intended application.

Many tissue adhesives—especially conventional surgical sealants, such as fibrin glue—rely on a curing step to *become* sticky. Commercial packages of fibrin glue contain a solution of fibrinogen and a solution of thrombin that are loaded into a dual-barrel syringe.[1] Other prominent examples of tissue adhesives with two-component mixing and gelation include various synthetic hydrogels, which cross-link upon mixing.[2–5] Cyanoacrylate glues polymerize at the interface with tissue and rapidly solidify. Many one-component, light-cured tissue adhesives have been developed to simplify deposition and gain control over the timing of the curing step.[6–9] However, to allow for the curing step, the tissue adhesive precursors in all of these examples must be deposited as liquids onto the surgical site, resulting in difficult experiences for surgeons, especially in minimally invasive procedures where specialized applicators are required.[10,11] Inaccurate application may lead to longer surgery times or cause unforeseen complications, such as thromboembolism.[12,13]

Bioinspired and reactive surface chemistries have been widely studied to improve tissue adhesion. Some tissue adhesives incorporate functional groups to bond to tissue, such as dopamine via oxidation, chitosan via electrostatics, *N*-hydroxysuccinimide, which readily

reacts with amines in tissue, or oxidized dextran, also via amines.[14–17] However, the cohesive properties—especially rheology—of tissue adhesives are often overlooked. A particularly good example of this transition occurring is in the field of mussel-inspired chemistry, which increasingly studies the cohesive properties of the pH-sensitive L-DOPA– metal complexes formed within mussel plaques. These and other bioinspired principles can be used as inspiration for new adhesive materials.[18–21] Few synthetic tissue adhesives have cohesive properties tailored to promote strong adhesive bonding.

RESULTS AND DISCUSSION

To develop the PSTA, we investigated blends of poly(lactide-*co*-caprolactone) (PLCL), which is a biodegradable elastomer,[22] and poly(lactide-*co*-glycolide) (PLGA), which could be used to increase stiffness (Figure 1A). Distinct low molecular weight (LMW) and high molecular weight (HMW) distributions of PLCL (see gel permeation chromatography (GPC), Figure 1B,C) were used to modulate viscoelasticity. In this work, we show that the rheological properties of the blends, especially their creep compliance and $\tan(\delta)$, have a profound effect on their surface wettability and, subsequently, their tissue adhesion. The PSTA capitalizes on advances in the synthesis and processing of biodegradable elastomers, such as optimized random copolymer ratios[23,24] and polymer blends with modified thermal properties[25–29] or degradation rates.[30–32]

The components of the PSTA can be dissolved in acetone to yield a sprayable polymer solution (Figure 1A, inset). Blends of LMW PLCL and HMW PLCL, as well as blends of LMW PLCL with PLGA, were investigated. Sprayability allows the PSTA to be deposited directly to the surgical site as fibers using a solution blow spinning airbrush (Figure 1D).[33] It then forms a thin film on tissue after softening (film shown in atomic force microscopy, Figure 1E). Tissue adhesion, degradation, and mechanical properties were characterized to determine which polymer blends exhibited the strongest pressure-sensitive adhesion. Depending on whether HMW PLCL or PLGA was incorporated, the PSTA could be tuned to degrade at different speeds and with varying amounts of erosion, which in turn produced differences in intraperitoneal space adhesiogenicity and immune response.

To investigate the PSTA's ability to form a strong adhesive bond, we sprayed the PSTA onto cardiac tissue and applied a poly(tetrafluoroethylene) cardiac patch with compressive force. Pressure-sensitivity of the PSTA can be inferred from the effect that pressure application time has on adhesion strength (Figure 2A). LMW PLCL has inherently high wettability and tack on wet tissue, producing a strong adhesive bond in seconds. To compare the effects of using HMW additives to create a PSTA blend with mechanical integrity, either HMW PLCL or PLGA was blended at a 70:30 ratio of LMW PLCL to HMW additive. 70:30 blends of LMW and HMW PLCL produce adhesive bonds that are stable, significantly increasing in strength after 5 min of applied pressure. Figure 2B summarizes the short-term time course of adhesion for 4 blends of LMW and HMW PLCL, showing that for LMW PLCL alone the bond deteriorates within 5 min. Without HMW PLCL, adhesion peaks at 1 min after application and then decreases.

The sealing strength of the polymer blends in wound closure was tested by measuring the burst pressure of a sealed partial incision *ex vivo* on segments of porcine intestine (Figure 2C). LMW PLCL supplemented with PLGA outperforms the PLCL LMW/HMW blends in this form of testing because of its high resistance to inflationary forces. The PLGA reinforces the system without sacrificing adhesion, preventing cohesive failure (Figure 2D). This, in combination with the adhesion strength study (Figure 2A), suggests that PLCL LMW/HMW PSTA would perform best as a surgical glue because it is less likely to experience adhesive failure and has inherent tackiness. However, LMW PLCL reinforced with PLGA would make a superior surgical sealant because it has the stiffness and strength to withstand inflation and deformation forces. Ultimately, this study demonstrates that using a system of PLCL and PLGA allows for the production of adhesive blends with a wide range of mechanical properties and potential applications.

The viscoelasticity of the PSTA dictates its ability to quickly form adhesive bonds with high strength. We used shear rheology to determine the relative modulus and frequency-dependent viscoelasticity of the PSTA polymer blends. Blends with tack—especially those containing LMW PLCL—exhibit lower storage modulus (G') and loss modulus (G'') (Figure 3A). The ratio of G'' to G', plotted as $\tan(\delta)$, represents the relative influence of viscous and elastic behavior (Figure 3B); it captures the unique ability of these elastomeric polymer blends to be viscous on long time scales (corresponding to 0.1–5 Hz) and elastic on short time scales (5–100 Hz). Both 70:30 PSTA blends are shifted toward the viscous-dominated regime ($\tan(\delta) > 1$): this imbues them with the high wettability and compliance (Figure 3C) necessary to quickly form adhesive bonds under pressure (Figure 3D) that pure HMW polymer cannot. Surface properties were also investigated by measuring the water droplet contact angle (Figure S2), as surface energy may influence interface formation and wetting behavior.[34–37] Interestingly, the PLCL used here is relatively hydrophilic, producing contact angles less than 90° for all types. However, there are no significant differences between the various PLCL groups at the time of application, which suggests that excellent wetting properties of the LMW PLCL blend PSTAs are largely a function of viscoelasticity and mechanical properties.

Blends of synthetic rubber—such as polyisobutylene and poly(styrene–butadiene-styrene) block copolymers—and a phenolic tackifying resin have been widely used for pressure-sensitive adhesion to nontissue, dry surfaces in consumer products like sticky notes.[38,39] These pressure-sensitive adhesives (PSAs) have even been repurposed for topical applications, such as adhesive bandages. While synthetic rubber PSAs can adhere effectively to skin—which is dry and hydrophobic unlike the wet tissue surfaces of internal organs—they are nondegradable, have been shown to cause allergic dermatitis, and may strip the healing wound of new tissue.[40–44] Previous research has established that their strong pressure-sensitive adhesion is a feature of their viscoelasticity, especially those that possess a transition from viscous to elastic behavior at intermediate frequency.[45,46]

Incorporating the HMW component allows the PSTA to retain sufficient elasticity under sudden deformation to form a durable bond that does not succumb to weak disruptive forces (Figure 3E). PSA formulations typically feature an elastomer with a rubbery region whose glass transition temperature (T_g) is 40–70 °C less than the operating temperature and glassy

regions that resist flow.[47] In tension, the PLCL-based PSTA blends demonstrate high strain recovery (Figure 3F). The PLCL selected for the PSTA (70:30 L:CL ratio) possesses a T_g of approximately −10 °C (Figure S1), which is ideal given that the operating temperature is body temperature (37 °C). In comparison, PLGA, which is much stiffer, has a T_g of approximately 40 °C.

Biodegradation of synthetic polyesters *in vivo* is a function of both polymer chain cleavage due to hydrolysis and erosion of LMW aggregates. Simulated mass loss studies and gel permeation chromatography (GPC) were performed to quantify both aspects of biodegradation. PLGA (50:50 L:G) primarily undergoes bulk polymer chain cleavage (GPC, Figure 4A), with minimal mass loss due to erosion occurring over 28 days (Figure 4B). However, LMW PLCL completely erodes in 1 day, and HMW PLCL undergoes a combination of erosion and bulk degradation. Blends of these exhibit a range of degradation speeds, determined by the HMW component. PLGA can be used to create slow-eroding PSTAs: adhesive blends with the pressure-sensitive properties of LMW PLCL (see schematic, Figure 4B). Blends of LMW and HMW PLCL also have low stiffness and high failure strain throughout their degradation (Figure 4C,D). The synergy in desirable degradation rate, viscoelasticity, and high adhesive strength afforded by a 70:30 blend of LMW and HMW PLCL is illustrated by Figure 4E, which consists of a logarithmic regression model (Figure S3) of adhesion strength versus time and tan(δ).

The sprayable PSTA can be delivered directly to the surgical site, allowing for custom fabrication of adhesive layers. It produces an initially porous mat that can span wounds (Figure 5Ai,ii). This adhesive layer can be used to secure a small biomedical device, such as a cardiac patch (Figure 5Aiii). When removed, the PSTA exhibits strong adhesion to both surfaces (Figure 5Aiv), dissipating a high amount of energy through stretching before detachment (Figure 5Av). The PSTA layer remains sticky after detachment but leaves little to no residue.

To determine the potential immune response to the fast-degrading components of the PSTA, we employed an intraperitoneal space implantation mouse model that can be used to evaluate fibrosis.[48,49] Surprisingly, PSTAs composed exclusively of PLCL produced fewer cases of fibrotic adhesions to the fat pads at 3 and 10 days than those that incorporated PLGA (Figure 5B). In the context of implanted materials, fibrosis may occur either (1) due to chronic inflammation in response to the implanted material or (2) due to acute inflammation from the wound healing response to surgical trauma that inhibits fibrinolysis.[50–54]

Interestingly, polymer degradation rate and mode play a critical role in the formation of fibrotic adhesions in this model. Each implant sample was also examined for fragmentation, which indicates high levels of erosion during degradation (Figure 5B). Those that degrade quickly, and primarily via erosion, like LMW PLCL, produced no adhesions to the fat pad; the implant itself degrades into soft fragments which could be found in the intraperitoneal space (Figure S4). PLGA implants, which primarily degrade via bulk chemical degradation, can be found intact (Figure S4), and were more frequently associated with adhesions to the abdominal fat pads or other organs.

Serum levels of tumor necrosis factor-α (TNF-α) and interferon-γ (IFN-γ) were also determined (Figure 5C,D). TNF-α and IFN-γ were rarely significantly different between the saline-injected sham procedure and other treatments, except in cases where the serum of the polymer-treated mice had decreased levels. The only case of elevated TNF-α compared to saline injection was for PLGA, which may be connected to the more severe immune response that coincides with fibrosis. This reduction in fibrosis when using PLCL-based PSTA blends suggests that it may be possible to reduce fibrotic adhesions using polymer blending strategies that promote erosion. Previous studies have also shown that viscoelasticity itself may affect cell adhesion.[55]

CONCLUSION

By blending LMW and HMW biodegradable polyesters, we formulated adhesives demonstrating a range of viscoelastic properties, from stiff and elastic to stretchy and resilient. Using elastomeric PLCL allowed for strong, pressure-sensitive bonding to occur with soft, hydrated tissue substrates, yielding a sprayable PSTA that is sticky without the need for curing. We further investigated the biodegradation and *in vivo* immune response toward these polymers, revealing interesting connections between degradation mechanisms and the tendency of intraperitoneal adhesions to form between the adhesive and surrounding organs such as the cecum or abdominal fat pad, as seen in our mouse model. Fast-degrading PSTAs composed of LMW and HMW PLCL have the potential to be used as temporary, biodegradable internal tissue adhesives with excellent flexibility during biodegradation and reduced potential for complications.

Supplementary Material

Refer to Web version on PubMed Central for supplementary material.

ACKNOWLEDGMENTS

REFERENCES

(1). Mandell SP; Gibran NS Fibrin Sealants: Surgical Hemostat, Sealant and Adhesive. Expert Opin. Biol. Ther 2014, 14 (6), 821–830. [PubMed: 24625330]

(2). Cencer M; Liu Y; Winter A; Murley M; Meng H; Lee BP Effect of PH on the Rate of Curing and Bioadhesive Properties of Dopamine Functionalized Poly(Ethylene Glycol) Hydrogels. Bio-macromolecules 2014, 15 (8), 2861–2869.

(3). Barrett DG; Bushnell GG; Messersmith PB Mechanically Robust, Negative-Swelling, Mussel-Inspired Tissue Adhesives. Adv. Healthcare Mater 2013, 2 (5), 745–755.

(4). Konieczynska MD; Villa-Camacho JC; Ghobril C; Perez-Viloria M; Tevis KM; Blessing WA; Nazarian A; Rodriguez EK; Grinstaff MW On-Demand Dissolution of a Dendritic Hydrogel-Based Dressing for Second-Degree Burn Wounds through Thiol-Thioester Exchange Reaction. Angew. Chem., Int. Ed 2016, 55 (34), 9984–9987.

(5). Bu Y; Zhang L; Sun G; Sun F; Liu J; Yang F; Tang P; Wu D Tetra-PEG Based Hydrogel Sealants for In Vivo Visceral Hemostasis. Adv. Mater 2019, 31 (28), 1901580.

(6). Annabi N; Zhang Y-N; Assmann A; Sani ES; Cheng G; Lassaletta AD; Vegh A; Dehghani B; Ruiz-Esparza GU; Wang X; Gangadharan S; Weiss AS; Khademhosseini A Engineering a Highly Elastic Human Protein-Based Sealant for Surgical Applications. Sci. Transl. Med 2017, 9 (410), No. eaai7466. [PubMed: 28978753]

(7). Annabi N; Rana D; Shirzaei Sani E; Portillo-Lara R; Gifford JL; Fares MM; Mithieux SM; Weiss AS Engineering a Sprayable and Elastic Hydrogel Adhesive with Antimicrobial Properties for Wound Healing. Biomaterials 2017, 139, 229–243. [PubMed: 28579065]

(8). Alleyne CH; Cawley CM; Barrow DL; Poff BC; Powell MD; Sawhney AS; Dillehay DL Efficacy and Biocompatibility of a Photopolymerized, Synthetic, Absorbable Hydrogel as a Dural Sealant in a Canine Craniotomy Model. J. Neurosurg 1998, 88 (2), 308–313. [PubMed: 9452241]

(9). Lang N; Pereira MJ; Lee Y; Friehs I; Vasilyev NV; Feins EN; Ablasser K; O'Cearbhaill ED; Xu C; Fabozzo A; Padera R; Wasserman S; Freudenthal F; Ferreira LS; Langer R; Karp JM; del Nido PJ A Blood-Resistant Surgical Glue for Minimally Invasive Repair of Vessels and Heart Defects. Sci. Transl. Med 2014, 6 (218), 218ra6.

(10). Lee M-GM; Jones D Applications of Fibrin Sealant in Surgery. Surg. Innov 2005, 12 (3), 203–213. [PubMed: 16224640]

(11). Heher P; Ferguson J; Redl H; Slezak P An Overview of Surgical Sealant Devices: Current Approaches and Future Trends. Expert Rev. Med. Devices 2018, 15 (10), 747–755. [PubMed: 30295541]

(12). Samudrala S Topical Hemostatic Agents in Surgery: A Surgeon's Perspective. AORN J. 2008, 88 (3), S2–S11. [PubMed: 18790097]

(13). Spotnitz WD Commercial Fibrin Sealants in Surgical Care. Am. J. Surg 2001, 182 (2), S8–S14.

(14). Liu Y; Meng H; Qian Z; Fan N; Choi W; Zhao F; Lee BP A Moldable Nanocomposite Hydrogel Composed of a Mussel-Inspired Polymer and a Nanosilicate as a Fit-to-Shape Tissue Sealant. Angew. Chem., Int. Ed 2017, 56 (15), 4224–4228.

(15). Li J; Celiz AD; Yang J; Yang Q; Wamala I; Whyte W; Seo BR; Vasilyev NV; Vlassak JJ; Suo Z; Mooney DJ Tough Adhesives for Diverse Wet Surfaces. Science 2017, 357 (6349), 378–381. [PubMed: 28751604]

(16). Strehin I; Nahas Z; Arora K; Nguyen T; Elisseeff J A Versatile PH Sensitive Chondroitin Sulfate-PEG Tissue Adhesive and Hydrogel. Biomaterials 2010, 31 (10), 2788–2797. [PubMed: 20047758]

(17). Artzi N; Shazly T; Crespo C; Ramos AB; Chenault HK; Edelman ER Characterization of Star Adhesive Sealants Based On PEG/Dextran Hydrogels. Macromol. Biosci 2009, 9 (8), 754–765. [PubMed: 19384975]

(18). Ahn BK Perspectives on Mussel-Inspired Wet Adhesion. J. Am. Chem. Soc 2017, 139 (30), 10166–10171. [PubMed: 28657746]

(19). Yang B; Lim C; Hwang DS; Cha HJ Switch of Surface Adhesion to Cohesion by Dopa-Fe3+ Complexation, in Response to Microenvironment at the Mussel Plaque/Substrate Interface. Chem. Mater 2016, 28 (21), 7982–7989.

(20). Anderson TH; Yu J; Estrada A; Hammer MU; Waite JH; Israelachvili JN The Contribution of DOPA to Substrate-Peptide Adhesion and Internal Cohesion of Mussel-Inspired Synthetic Peptide Films. Adv. Funct. Mater 2010, 20 (23), 4196–4205. [PubMed: 21603098]

(21). Pena-Francesch A; Akgun B; Miserez A; Zhu W; Gao H; Demirel MC Pressure Sensitive Adhesion of an Elastomeric Protein Complex Extracted From Squid Ring Teeth. Adv. Funct. Mater 2014, 24 (39), 6227–6233.

(22). Jeong SI; Kim SH; Kim YH; Jung Y; Kwon JH; Kim B-S; Lee YM Manufacture of Elastic Biodegradable PLCL Scaffolds for Mechano-Active Vascular Tissue Engineering. J. Biomater. Sci., Polym. Ed 2004, 15 (5), 645–660. [PubMed: 15264665]

(23). Mir M; Ahmed N; Rehman A. ur. Recent Applications of PLGA Based Nanostructures in Drug Delivery. Colloids Surf., B 2017, 159, 217–231.

(24). Jeong SI; Kim B-S; Kang SW; Kwon JH; Lee YM; Kim SH; Kim YH In Vivo Biocompatibilty and Degradation Behavior of Elastic Poly(l-Lactide-Co-ɛ;-Caprolactone) Scaffolds. Biomaterials 2004, 25 (28), 5939–5946. [PubMed: 15183608]

(25). Saini P; Arora M; Kumar MNVR Poly(Lactic Acid) Blends in Biomedical Applications. Adv. Drug Delivery Rev 2016, 107, 47–59.

(26). Li T; Zhang J; Schneiderman DK; Francis LF; Bates FS Toughening Glassy Poly(Lactide) with Block Copolymer Micelles. ACS Macro Lett. 2016, 5 (3), 359–364.

(27). Behrens AM; Lee NG; Casey BJ; Srinivasan P; Sikorski MJ; Daristotle JL; Sandler AD; Kofinas P Biodegradable-Polymer-Blend-Based Surgical Sealant with Body-Temperature-Mediated Adhesion. Adv. Mater 2015, 27 (48), 8056–8061. [PubMed: 26554545]

(28). Daristotle JL; Lau LW; Erdi M; Hunter J; Djoum A; Srinivasan P; Wu X; Basu M; Ayyub OB; Sandler AD; Kofinas P Sprayable and Biodegradable, Intrinsically Adhesive Wound Dressing with Antimicrobial Properties. Bioeng. Transl. Med 2020, 5 (1), No. e10149. [PubMed: 31989038]

(29). Kobayashi J; Okano T Design of Temperature-Responsive Polymer-Grafted Surfaces for Cell Sheet Preparation and Manipulation. Bull. Chem. Soc. Jpn 2019, 92 (4), 817–824.

(30). Lao LL; Venkatraman SS; Peppas NA Modeling of Drug Release from Biodegradable Polymer Blends. Eur. J. Pharm. Biopharm 2008, 70 (3), 796–803. [PubMed: 18577449]

(31). Imre B; Pukanszky B Compatibilization in Bio-Based and Biodegradable Polymer Blends. Eur. Polym. J 2013, 49 (6), 1215–1233.

(32). Behrens AM; Kim J; Hotaling N; Seppala JE; Kofinas P; Tutak W Rapid Fabrication of Poly(DL-Lactide) Nanofiber Scaffolds with Tunable Degradation for Tissue Engineering Applications by Air-Brushing. Biomed. Mater 2016, 11 (3), 035001. [PubMed: 27121660]

(33). Daristotle JL; Behrens AM; Sandler AD; Kofinas P A Review of the Fundamental Principles and Applications of Solution Blow Spinning. ACS Appl. Mater. Interfaces 2016, 8 (51), 34951–34963. [PubMed: 27966857]

(34). Good RJ Contact Angle, Wetting, and Adhesion: A Critical Review. J. Adhes. Sci. Technol 1992, 6 (12), 1269–1302.

(35). Li L; Tirrell M; Korba GA; Pocius AV Surface Energy and Adhesion Studies on Acrylic Pressure Sensitive Adhesives. J. Adhes 2001, 76 (4), 307–334.

(36). Kowalski A; Czech Z The Effects of Substrate Surface Properties on Tack Performance of Acrylic Pressure-Sensitive Adhesives (PSAs). Int. J. Adhes. Adhes 2015, 60, 9–15.

(37). Karnal P; Roberts P; Gryska S; King C; Barrios C; Frechette J Importance of Substrate Functionality on the Adhesion and Debonding of a Pressure-Sensitive Adhesive under Water. ACS Appl. Mater. Interfaces 2017, 9 (48), 42344–42353. [PubMed: 29111640]

(38). Deng X Progress on Rubber-Based Pressure-Sensitive Adhesives. J. Adhes 2018, 94 (2), 77–96.

(39). Shin J; Martello MT; Shrestha M; Wissinger JE; Tolman WB; Hillmyer MA Pressure-Sensitive Adhesives from Renewable Triblock Copolymers. Macromolecules 2011, 44 (1), 87–94.

(40). Rippon M; White R; Davies P Skin Adhesives and Their Role in Wound Dressings. Wounds UK 2007, 3 (4), 76–86.

(41). Widman TJ; Oostman H; Storrs FJ Allergic Contact Dermatitis from Medical Adhesive Bandages in Patients Who Report Having a Reaction to Medical Bandages: Dermatitis 2008, 19 (1), 32–37. [PubMed: 18346394]

(42). King A; Stellar JJ; Blevins A; Shah KN Dressings and Products in Pediatric Wound Care. Adv. Wound Care 2014, 3 (4), 324–334.

(43). Waring M; Bielfeldt S; Mätzold K; Wilhelm KP; Butcher M An Evaluation of the Skin Stripping of Wound Dressing Adhesives. J. Wound Care 2011, 20 (9), 412–422. [PubMed: 22068140]

(44). Wiegand C; Abel M; Hipler U-C; Elsner P Effect of Non-Adhering Dressings on Promotion of Fibroblast Proliferation and Wound Healing in Vitro. Sci. Rep 2019, 9 (1), 1–10. [PubMed: 30626917]

(45). Mazzeo FA Characterization of Pressure Sensitive Adhesives by Rheology. TA Instrum. Rep. RH082 2002, 1–8.

(46). Vendamme R; Schüwer N; Eevers W Recent Synthetic Approaches and Emerging Bio-Inspired Strategies for the Development of Sustainable Pressure-Sensitive Adhesives Derived from Renewable Building Blocks. J. Appl. Polym. Sci 2014, 131 (17), 40669.

(47). Creton C; Hu G; Deplace F; Morgret L; Shull KR Large-Strain Mechanical Behavior of Model Block Copolymer Adhesives. Macromolecules 2009, 42 (20), 7605–7615.

(48). Doloff JC; Veiseh O; Vegas AJ; Tam HH; Farah S; Ma M; Li J; Bader A; Chiu A; Sadraei A; Aresta-Dasilva S; Griffin M; Jhunjhunwala S; Webber M; Siebert S; Tang K; Chen M; Langan E; Dholokia N; Thakrar R; Qi M; Oberholzer J; Greiner DL; Langer R; Anderson DG Colony Stimulating Factor-1 Receptor Is a Central Component of the Foreign Body Response to Biomaterial Implants in Rodents and Non-Human Primates. Nat. Mater 2017, 16 (6), 671. [PubMed: 28319612]

(49). Daristotle JL; Zaki ST; Lau LW; Torres L; Zografos A; Srinivasan P; Ayyub OB; Sandler AD; Kofinas P Improving the Adhesion, Flexibility, and Hemostatic Efficacy of a Sprayable Polymer Blend Surgical Sealant by Incorporating Silica Particles. Acta Biomater. 2019, 90, 205–216. [PubMed: 30954624]

(50). Menzies D Postoperative Adhesions: Their Treatment and Relevance in Clinical Practice. Ann. R. Coll. Surg. Engl 1993, 75 (3), 147–153.

(51). Arung W; Meurisse M; Detry O Pathophysiology and Prevention of Postoperative Peritoneal Adhesions. World J. Gastro-enterol. WJG 2011, 17 (41), 4545–4553.

(52). Kamel RM Prevention of Postoperative Peritoneal Adhesions. Eur. J. Obstet. Gynecol. Reprod. Biol 2010, 150 (2), 111–118. [PubMed: 20382467]

(53). Maciver AH; McCall M; James Shapiro AM Intra-Abdominal Adhesions: Cellular Mechanisms and Strategies for Prevention. Int. J. Surg 2011, 9 (8), 589–594. [PubMed: 21964216]

(54). Brüggmann D; Tchartchian G; Wallwiener M; Münstedt K; Tinneberg H-R; Hackethal A Intra-Abdominal Adhesions. Dtsch. Ärztebl. Int 2010, 107 (44), 769–775. [PubMed: 21116396]

(55). Ariga K; Jia X; Song J; Hsieh C-T; Hsu S Materials Nanoarchitectonics as Cell Regulators. ChemNanoMat 2019, 5 (6), 692–702.
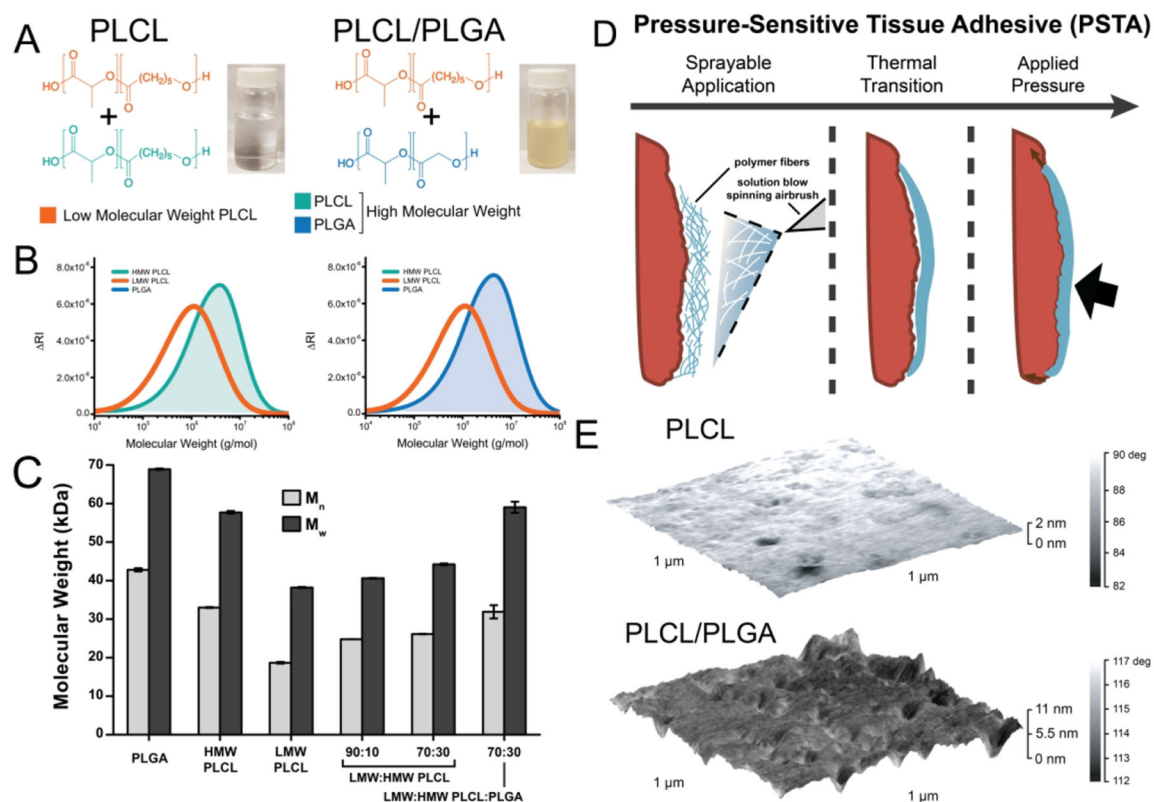
Figure 1.
Components (A, B) and gel permeation chromatography (C) of the tissue adhesive polymer blends. (D) Schematic of sprayable pressure-sensitive tissue adhesive (PSTA) deposition, and (E) atomic force microscopy of the PSTA surface.
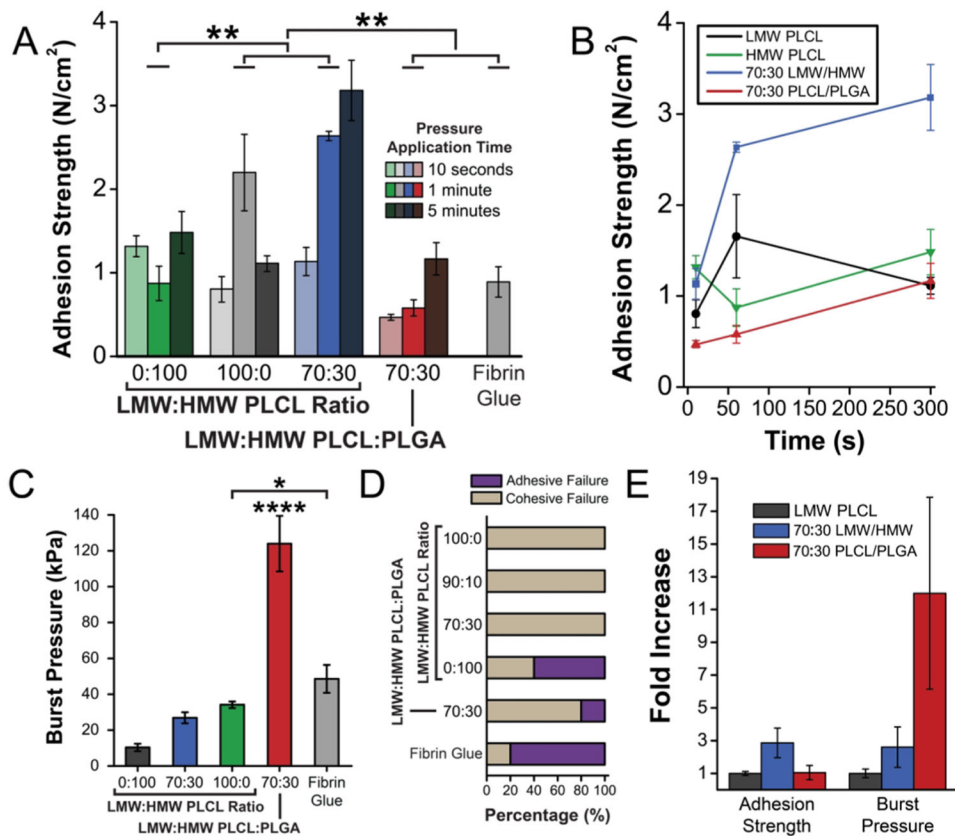
Figure 2.
(A) Cardiac-patch-to-cardiac-tissue adhesion strength of various blends of poly(lactide-*co*-caprolactone) (PLCL) and poly (lactide-*co*-glycolide) (PLGA) and fibrin glue after 10 s, 1 min, and 5 min of applied pressure. (B) Adhesion strength versus application time for pressure-sensitive polymer blends, showing the continued increase in adhesion when a blend of LMW and HMW polymers are used. (C) *Ex vivo* burst pressure on intestine using only the adhesive as a sealant, (D) with failure mode reported. (E) Factor increase in adhesion strength or burst pressure, showing the difference in effect of PLCL and PLGA as HMW blend components.
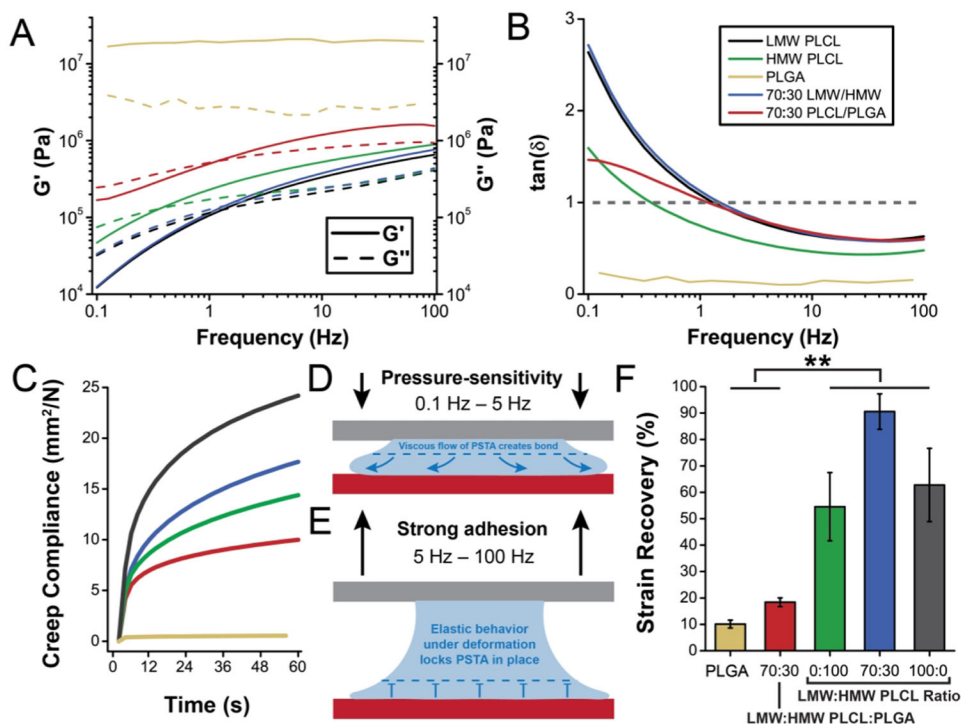
Figure 3.
(A, B) Shear rheology of polymer blends, showing the shift toward elastic, solidlike properties with HMW polymers. Storage (G') and loss (G'') modulus (A) across a frequency range encompassing long time scales relevant for pressure-sensitive bond formation (0.1–5 Hz) and short time scales relevant for high bond strength and adhesion after application (5 Hz–100 Hz). (B) Plot of tan(δ) highlights the frequency-dependent shift at 1 Hz in viscoelasticity necessary for pressure-sensitive tissue adhesion. (C) Creep compliance of polymer blends in compression. The combination of viscosity and elasticity present in the polymer blends allows for pressure-sensitivity (D) and strong adhesion (E), respectively.(F) Strain recovery in tension for various polymer blends.
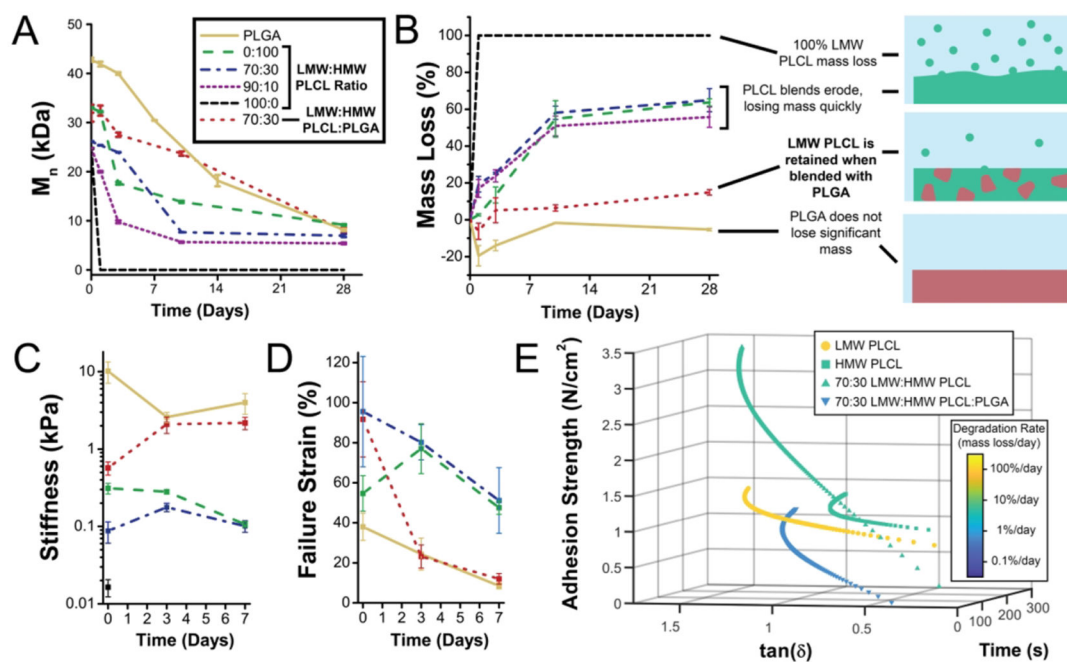
Figure 4.
Gel permeation chromatography (GPC) (A), mass loss (B), tensile stiffness (C), and failure strain (D) of polymer blend adhesives during *in vitro* degradation. (E) Three-dimensional regression plot of time, adhesion strength, and tan(δ) showing the interplay between degradation, rheology, and pull-off tissue adhesion.
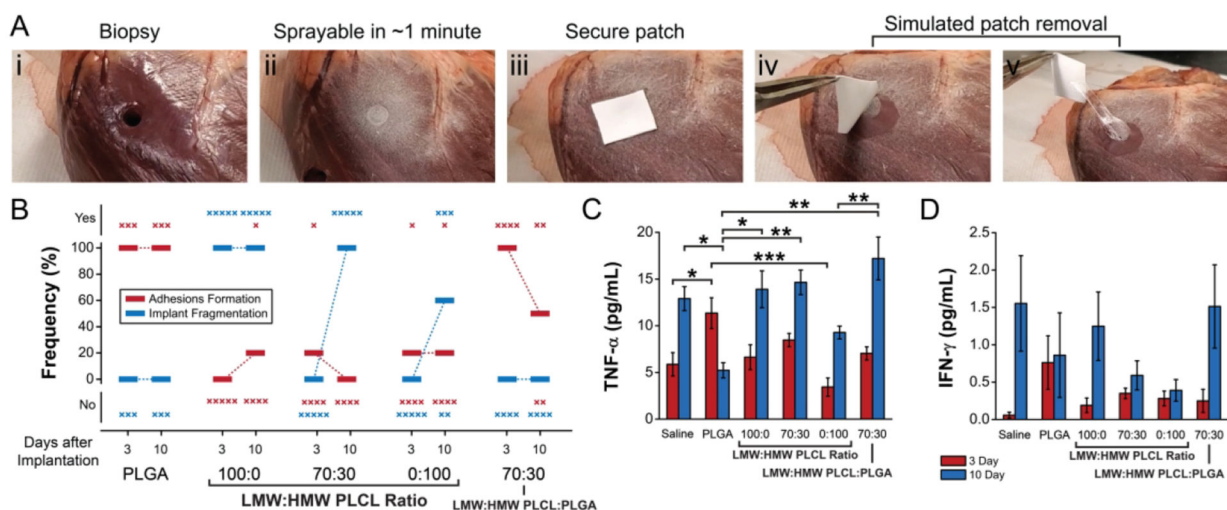
Figure 5.
Application strategy for sprayable pressure-sensitive tissue adhesive (PSTA) and immune response toward PSTA components. PSTA can be sprayed directly onto a biopsy site (Ai), forming a thin coherent layer in approximately 1 min (Aii). A cardiac patch can be secured to the biopsy site by applying pressure (Aiii). During patch removal, the adhesive produces a strong bond (Aiv) with high energy dissipation through material stretching and cracking prior to failure (Av). (B) Frequency of fibrotic adhesions to the fat pads and implant fragmentation for polymers implanted in the intraperitoneal space of a mouse model, at 3 and 10 days postsurgery. Serum levels of tumor necrosis factor-α (TNF-α) (C) and interferon-γ (IFN-γ) (D) for the same model.